Available online at www.sciencedirect.com
ScienceDirect
Journal of Sound and Vibration 301 (2007) 950–962
JOURNAL OF SOUND AND VIBRATION
www.elsevier.com/locate/jsvi

Stability analysis of doubly regenerative cylindrical grinding process

Zhaoheng Liu[a,*], Guy Payre[b]

[a]Department of Mechanical Engineering, École de Technologie Supérieure, Université du Québec, Montreal, Que., Canada H3C 1K3
[b]Department of Mechanical Engineering, Université de Sherbrooke, Sherbrooke, Que., Canada J1K 2R1

Received 15 August 2005; received in revised form 25 September 2006; accepted 31 October 2006
Available online 26 December 2006

Abstract

In this paper, we investigate the stability properties of a cylindrical grinding process. The dynamical model of the process includes two inherent delayed forcing terms, one from workpiece regeneration and the other from grinding wheel regeneration. The prediction of chatter onset is carried out by computing the spectrum of the doubly delayed differential equations for any set of physical and operational parameters. Stability diagrams are plotted in parameter space. The stability behavior obtained from this analysis is verified to be consistent with direct simulation results. A sensitivity analysis approach is also proposed, and can be used to lead an unstable process to a stable state by optimally varying one of the operational parameters.

1. Introduction

Grinding is an abrasive process often accompanied by an unwanted instability, called regenerative chatter. The problem of grinding chatter vibration is one of the factors that limit the productivity of many production operations. Modeling the dynamics of grinding operations is particularly intriguing because, unlike other machining processes, it involves significant dynamic variations in the shape of both the workpiece and the grinding wheel [1]. Furthermore, many grinding operations involve a driven motion of both the tool and the workpiece. This introduces a second delayed forcing term into the equations of motion of the system, rendering even the linear stability conditions very difficult to calculate. This doubly regenerative coupled problem has been the subject of several previous research studies [2–10]. Thompson published a series of papers [2–5] in which the chatter growth in cylindrical grinding was investigated. In his work, the normal grinding force between the workpiece and the tool was modeled as an exponential function of time to describe the exponential growth or decay of the chatter amplitude. His theory and analysis can be used to adjust wheel speed to optimize grinding time and establish a wheel dressing schedule. Recently, Yuan, Järvenpää, Keskinen and Cotsaftis [6–9] investigated the paper machine roll grinding process to detect the main characteristics of the system and to determine the key parameters that influence the stability. In Refs. [6–9], multi-body dynamic

*Corresponding author. Tel.: +1 514 396 8507; fax: +1 514 396 8530.
E-mail address: zhaoheng.liu@etsmtl.ca (Z. Liu).

0022-460X/$ - see front matter © 2006 Elsevier Ltd. All rights reserved.
doi:10.1016/j.jsv.2006.10.041

models were established and the system behavior was analyzed by using a numerical simulation strategy. Their simulations illustrated the influence of the delay effect on system dynamics. The Guan–Irons reduction method has also been used by Yuan et al. [7] to uncouple the multi-degree-of-freedom model into two separated equations. Each uncoupled equation includes only one time-delay, and traditional linear stability theory was used to investigate the behavior of each uncoupled system separately. Orynski and Pawlowski [11] reported the results of their work on the forced vibration damping of a wheelhead of a cylindrical grinder; their findings were based on simulation and experimental research.

Several recent research papers have also been published on the stability analysis of multiple time delayed dynamic systems. Bélaire and Campbell [12] considered a differential equation with two time delays and investigated the stability and bifurcations of the equilibria in a particular system. Their approach provided an insight into the stability regions in parameter space and the system's dynamical evolution as one privileged parameter is altered. Hu and Wang [13] proposed algorithms to find delay-independent stability criteria for a single-degree-of-freedom damped vibrating system with two time delays in state feedback. A comprehensive software package called DDE-BIFTOOL [14] is also freely available for scientific use; this Matlab package can be used for the numerical analysis of delayed differential systems with several fixed, discrete delays. It implements a continuation of steady-state solutions and periodic solutions as well as their stability analysis.

In this paper, we propose a practical algorithm for the stability analysis of dynamical systems with two time delays. The stability behavior is characterized by a localization of the system eigenvalues. We then apply this algorithm to investigate the stability behavior of a cylindrical grinding process, a doubly regenerative differential system. Thus, both the time delays and their coupling effect are taken into account simultaneously in the analysis. The main aim of the research reported in this paper was to locate the parameter values at the onset of the chatter vibration in the cylindrical grinding process. The remainder of this paper is structured as follows. The dynamical model with two time delays for the grinding process is briefly described in Section 2. In Section 3, the time-domain response obtained from the numerical integration of the system equations for stable or unstable motions, with and without perturbations (i.e. surface irregularities of the workpiece and the grinding wheel) is shown. The numerical method for analyzing stability by computing the eigenvalues of the autonomous system (using a labeling of the complex plane) is given in Section 4. In Section 5, stability diagrams are plotted using the method proposed in Section 4. In Section 6 is a description of how it may be possible to bring an unstable system to a stable state as quickly as possible by properly adjusting the operational parameters. We conclude finally with some general remarks on our contributions and on the usefulness of these concepts in the stability characterization of a cylindrical grinding process.

2. Mathematical model of the grinding process

The dynamics of a roll grinding process [6] is considered here. The workpiece (w) is a long cylindrical roll (mass m_w) rotating at a constant angular speed, ω_w. The grinding wheel mechanism (mass m_g) is attached to a sledge parallel to the roll axis and pushed against the roll by a cutting force F_N (see Fig. 1). The grinding wheel

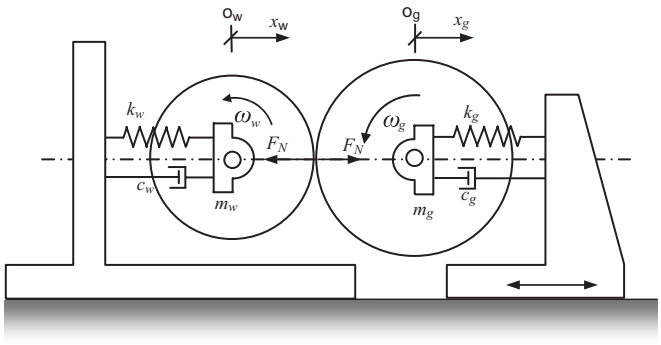

Fig. 1. Dynamic model of roll grinding operation [1].

rotates at a high speed, ω_g, and also moves horizontally along the roll at a slow translational speed, v_g. The whole system may be described through an equivalent spring-mass model [1] illustrated in Fig. 1, which obeys the following differential equations:

$$\begin{aligned} m_g\ddot{x}_g + c_g\dot{x}_g + k_g x_g &= F_N, \\ m_w\ddot{x}_w + c_w\dot{x}_w + k_w x_w &= -F_N. \end{aligned} \tag{1}$$

In this paper, the grinding model described in Ref. [7] for the normal contact force F_N at the grinding point is used:

$$F_N(t) = k_N([\varepsilon_w(t) - \alpha\varepsilon_w(t-\tau_w)] - [\varepsilon_g(t) - \varepsilon_g(t-\tau_g)]), \tag{2}$$

where k_N is a contact stiffness between the roll and the grinding stone ($\varepsilon_g, \varepsilon_w$) are, respectively, the depths of penetration into the grinding wheel and into the roll and

$$\alpha = 1 - 2\pi\frac{v_g}{W\omega_w}, \tag{3}$$

is an overlapping factor related to the width W of the wheel.

In some circumstances, which will be described below, the grinding operation may lose its stable behavior and begin to "chatter", leading to an undesirable surface finish and a tool life shortening. In regenerative feedback theory [2] it has been shown that the two time delays, $\tau_g = 2\pi/\omega_g$ and $\tau_w = 2\pi/\omega_w$ play a major role in the onset of chatter. Let us remark here that $\omega_g > \omega_w$, such that $\tau_g < \tau_w$.

As indicated in Ref. [7], sinusoidal error patterns exist on the surfaces of the roll and of the grinding wheel. This sinusoidal defect on the workpiece is made of n_w waves of amplitude Δ_R, such that the depth of penetration into the workpiece is related to the roll displacement, $x_w(t)$, by the equation

$$\varepsilon_w(t) = x_w(t) - \Delta_R \sin(n_w\omega_w t) + x_{f_w}. \tag{4}$$

Assuming the same error pattern (amplitude Δ_r) on the grinding wheel, and taking into account the direction of the x-axis and the opposite rotation of the grinder, the corresponding depth of penetration into the grinding wheel is computed by

$$\varepsilon_g(t) = x_g(t) + \Delta_r \sin(\pi - n_g\omega_g t) + x_{f_g}. \tag{5}$$

In these expressions, x_{f_g} and x_{f_w} stand for the constant cutting feed applied to the grinder and to the workpiece, respectively. Then, the contact force may be written as

$$\begin{aligned} F_N(t) = {} & k_N[x_w(t) - x_g(t)] - k_N[\alpha x_w(t-\tau_w) - x_g(t-\tau_g)] \\ & - k_N\Delta_R[\sin(n_w\omega_w t) - \alpha\sin(n_w\omega_w(t-\tau_w))] \\ & - k_N\Delta_r[\sin(\pi - n_g\omega_g t) - \sin(\pi - n_g\omega_g(t-\tau_g))] \\ & + k_N(1-\alpha)x_{f_w}. \end{aligned} \tag{6}$$

Let us associate Index 1 to the grinding wheel (g) and Index 2 to the workpiece (w). The two time delays (τ_1, τ_2) occurring in the differential system are now $\tau_1 = \tau_g = 2\pi/\omega_g, \tau_2 = \tau_w = 2\pi/\omega_w$, with $\tau_1 < \tau_2$. We define the state vector $\mathbf{y}(t)$ by $\mathbf{y}(t) = (x_1\ x_2\ \dot{x}_1\ \dot{x}_2)^{\mathrm{t}}$.

The differential system becomes $\dot{\mathbf{y}}(t) = \mathbf{f}(\mathbf{y}(t), \mathbf{y}(t-\tau_1), \mathbf{y}(t-\tau_2), t, \gamma)$ or, more precisely,

$$\dot{\mathbf{y}}(t) = \mathbf{A}_0(\gamma)\mathbf{y}(t) + \mathbf{A}_1(\gamma)\mathbf{y}(t-\tau_1) + \mathbf{A}_2(\gamma)\mathbf{y}(t-\tau_2) + \mathbf{p}(t,\gamma) + \mathbf{C}(\gamma), \tag{7}$$

where

$$\mathbf{A}_0 = \begin{pmatrix} 0 & 0 & 1 & 0 \\ 0 & 0 & 0 & 1 \\ -\dfrac{k_1+k_N}{m_1} & \dfrac{k_N}{m_1} & -\dfrac{c_1}{m_1} & 0 \\ \dfrac{k_N}{m_2} & -\dfrac{k_2+k_N}{m_2} & 0 & -\dfrac{c_2}{m_2} \end{pmatrix},$$

$$\mathbf{A}_1 = \begin{pmatrix} 0 & 0 & 0 & 0 \\ 0 & 0 & 0 & 0 \\ \dfrac{k_N}{m_1} & 0 & 0 & 0 \\ \dfrac{k_N}{m_2} & 0 & 0 & 0 \end{pmatrix}, \qquad \mathbf{A}_2 = \begin{pmatrix} 0 & 0 & 0 & 0 \\ 0 & 0 & 0 & 0 \\ 0 & -\dfrac{\alpha k_N}{m_1} & 0 & 0 \\ 0 & \dfrac{\alpha k_N}{m_2} & 0 & 0 \end{pmatrix},$$

$$\mathbf{p} = \{p_1, p_2, p_3, p_4\}^{\mathrm{t}}$$

where

$$p_1 = 0, \quad p_2 = 0,$$

$$p_3 = -\frac{k_N}{m_1}\{\Delta_r[\sin(\pi - n_g\omega_g t) - \sin(\pi - n_g\omega_g(t-\tau_1))] + \Delta_R[\sin(n_w\omega_w t) - \alpha\sin(n_w\omega_w(t-\tau_2))]\},$$

$$p_4 = \frac{k_N}{m_2}\{\Delta_r[\sin(\pi - n_g\omega_g t) - \sin(\pi - n_g\omega_g(t-\tau_1))] + \Delta_R[\sin(n_w\omega_w t) - \alpha\sin(n_w\omega_w(t-\tau_2))]\},$$

and

$$\mathbf{C} = \{C_1, C_2, C_3, C_4\}$$

where

$$C_1 = 0, \quad C_2 = 0, \quad C_3 = (1-\alpha)\frac{k_N}{m_1}x_{f_w}, \quad C_4 = -(1-\alpha)\frac{k_N}{m_2}x_{f_w}.$$

3. Stable and unstable states

In a first step, the differential system Eq. (7) is integrated in the time domain by a Runge–Kutta method of order 4 to illustrate the stable and unstable behaviors of the system. The numerical values of the physical parameters given in the appendix correspond to a typical roll grinding system [7]. The motions, $x_1(t)$ and $x_2(t)$, are set to zero for $-\tau_2 \leqslant t \leqslant 0$ and the load $F_N(t)$ applied afterwards for $t > 0$. The grinding wheel is operated at a frequency of 10 Hz ($\omega_g = 62.83$ rad/s), and is moving along the roll at a speed, $v_g = 0.0105$ m/s.

In Eqs. (4) and (5), sinusoidal error patterns are assumed to be present on the surfaces of the workpiece and grinding wheel. We used Δ_R and Δ_r to denote, respectively, the amplitude of the error waves for the workpiece and the grinding wheel. These surface imperfections exist inevitably in the material to be ground and in the grinder. In what follows, we will illustrate the system dynamical response in the time domain for two cases: the

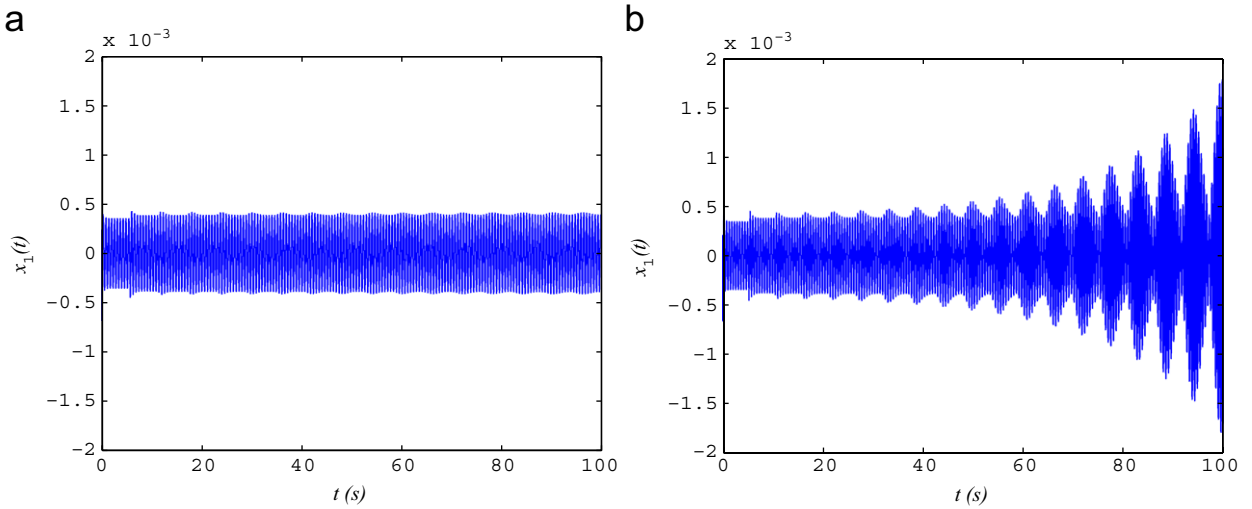

Fig. 2. Perturbed evolution: (a) stable and (b) unstable behavior.

perturbed system in which we assume that Δ_R and Δ_r are nonzero and the unperturbed system in which there is no surface imperfection ($\Delta_R = 0$ and $\Delta_r = 0$). In both cases, the system can become unstable when the workpiece rotational speed is set beyond a critical value.

3.1. *Perturbed system* ($\Delta_R, \Delta_r \neq 0$)

Depending on the rotational velocity of the roll, the system may exhibit stable oscillations or may enter into a vibratory mode of ever increasing amplitude. In Fig. 2(a), the evolution of the grinder displacement $x_1(t)$ for a value of $\omega_w = 1.1\,\mathrm{rad/s}$, corresponding to smooth grinding behavior is shown. For a small increase in the roll rotational speed to $\omega_w = 1.2\,\mathrm{rad/s}$, the amplitude of this oscillating displacement increases exponentially (Fig. 2(b)). This is in accord with the Thompson's chatter theory [2], where an exponentially increasing contact force $F_N(t)$ is associated with the onset of chatter. The contact force and the lateral vibration of the grinder behave similarly, as they are related by Eq. (1).

3.2. *Unperturbed system* ($\Delta_R, \Delta_r = 0$)

The unstable mode which appears in this case is not a consequence of growing surface irregularities, but is rather a cause of the exponential increase of these defects. The numerical integration of the same grinding system acting on perfectly rounded surfaces gives the results of Fig. 3, (a) for the stable case and (b) for the unstable one. It is noted that the scales of the vertical axes in Fig. 3(a) and (b) are different in order to show the oscillating behavior of the stable response clearly. The peak values of the unstable case can be extracted from the data, and a least-squares algorithm combined with a deferred correction to the limit is applied on these values in order to estimate the exponential rate of increase of the envelope at $t = 100s$. This process gives $\mathrm{Env}(|x_1(t)|) \approx x_{1,0}\,\mathrm{e}^{at}$ with $a = 5.05 \times 10^{-2}$, $x_{1,0} = 7.6 \times 10^{-6}$. The curve $\mathrm{Env}(|x_1(t)|)$ is plotted in Fig. 3(b). In fact, we have found that, at least for this particular set of system parameters, this exponential rate of increase is directly related to the eigenvalues of the system as described later in Section 5.

One can notice that the system responses illustrated in Figs. 2(b) 3(b) correspond to unstable cases where the behavior is purely exponential without saturation. In reality, the nonlinearities can bring an effect of saturation which limits the vibration amplitude to a finite value. However, the model Eq. (7) under study in this work is linear in terms of system state variables and the forcing terms, even nonlinear, will not cause an effect of saturation.

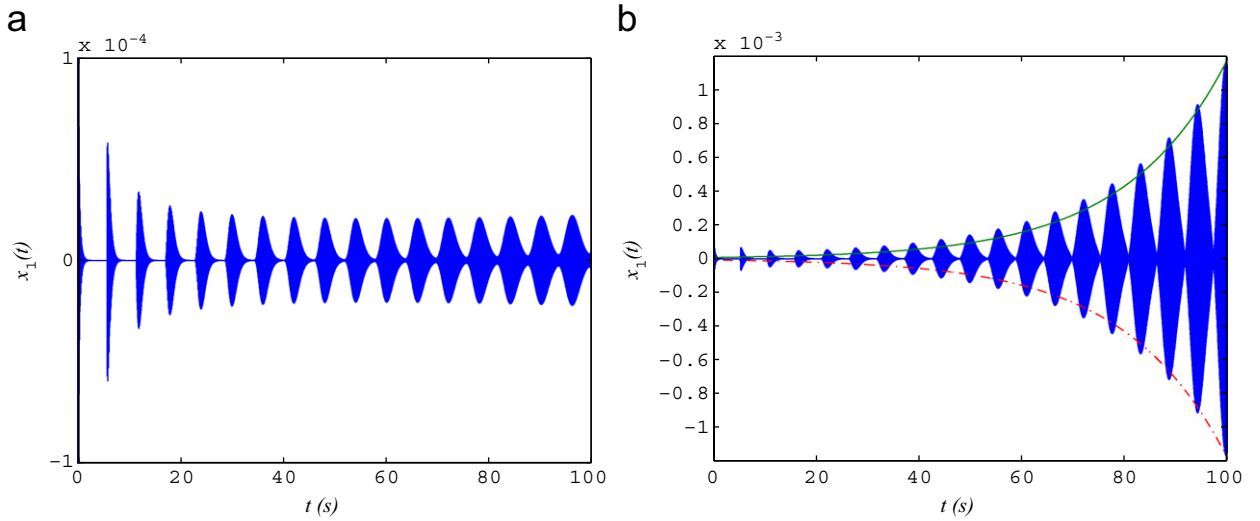

Fig. 3. Unperturbed evolution: (a) stable and (b) unstable behavior.

4. System stability and eigenvalues

A stability analysis of the doubly delayed differential system is carried out in this section in order to precisely detect the onset of chatter for the case of the autonomous differential system:

$$\frac{\mathrm{d}y}{\mathrm{d}t} = \mathbf{A}_0\mathbf{y}(t) + \mathbf{A}_1\mathbf{y}(t-\tau_1) + \mathbf{A}_2\mathbf{y}(t-\tau_2). \tag{8}$$

Let us introduce the complex matrix $\hat{\mathbf{A}}(\lambda)$ computed by

$$\hat{\mathbf{A}}(\lambda) = \mathbf{A}_0 + \mathbf{A}_1\,\mathrm{e}^{-\tau_1\lambda} + \mathbf{A}_2\,\mathrm{e}^{-\tau_2\lambda}. \tag{9}$$

Then, the characteristic equation of the delayed differential system of Eq. (8) is expressed by

$$\Delta(\lambda) = \det[\lambda\mathbf{I} - \hat{\mathbf{A}}(\lambda)]. \tag{10}$$

In this particular case, the matrix $\lambda\mathbf{I} - \hat{\mathbf{A}}(\lambda)$ is not highly populated, and so this determinant can be easily computed:

$$\Delta(\lambda) = \lambda^4 + \theta_1\lambda^3 + \theta_2(\lambda)\lambda^2 + \theta_3(\lambda)\lambda + \theta_4(\lambda) \tag{11}$$

with

$$\begin{aligned}
\theta_1 &= \frac{m_1c_2 + m_2c_1}{m_1m_2},\\
\theta_2 &= \frac{m_1(k_2+k_N) + m_2(k_1+k_N) + c_1c_2}{m_1m_2} - \frac{k_N}{m_1}\mathrm{e}^{-\tau_1\lambda} - \frac{\alpha k_N}{m_2}\mathrm{e}^{-\tau_2\lambda},\\
\theta_3 &= \frac{c_1(k_2+k_N) + c_2(k_1+k_N)}{m_1m_2} - \frac{c_2k_N}{m_1m_2}\mathrm{e}^{-\tau_1\lambda} - \frac{\alpha c_1k_N}{m_1m_2}\mathrm{e}^{-\tau_2\lambda},\\
\theta_4 &= \frac{k_1k_2 + k_1k_N + k_2k_N}{m_1m_2} - \frac{k_2k_N}{m_1m_2}\mathrm{e}^{-\tau_1\lambda} - \frac{\alpha k_1k_N}{m_1m_2}\mathrm{e}^{-\tau_2\lambda}.
\end{aligned} \tag{12}$$

The eigenvalues of the delayed differential system are given by the roots of the function $\Delta(\lambda)$. These roots are known to be of finite multiplicity with upper bounded real parts. They appear in conjugate pairs that are symmetrical with respect to the real axis. For the system to be stable, all the eigenvalues must lie in the left-hand side part of the complex plane (the real parts must be negative). The localization of these eigenvalues can be achieved by a numerical method based on the labeling of a bounded region in the complex plane [15,16], as briefly explained next.

Let $f(z)$ denote an entire function of z. Define L_z, the label of z, as

$$L_z = \begin{cases} 1 & \text{for } -\pi/3 \leqslant \arg(f(z)) \leqslant \pi/3 \quad \text{or} \quad \text{if } f(z) = 0, \\ 2 & \text{for } \pi/3 < \arg(f(z)) \leqslant \pi, \\ 3 & \text{for } -\pi < \arg(f(z)) < -\pi/3. \end{cases} \tag{13}$$

Let (z_1, z_2, z_3) be a triple of complex numbers. An edge (z_i, z_j) is said to be *distinct* if $L_{z_i} \neq L_{z_j}$. A triangle with three distinct edges is said to be *saturated*, which implies that the set $\{L_{z_1}, L_{z_2}, L_{z_3}\}$ is identical to $\{1, 2, 3\}$. The continuity property of the function f ensures that ε-small saturated triangles can only be found near a zero of f. Hence, the problem of finding the zeros of $f(z)$ in a given bounded region can be tackled by constructing a subdivision of the region into triangles and finding the saturated ones.

In practice, one takes a rectangular region B and constructs a grid. The mesh points of the grid are then searched for saturated triples of neighbors. Searching all the points of the grid would result in an $O(n^2)$ algorithm, and this may be avoided by remarking that a triangle cannot have only one distinct edge, and proceeding along the following steps:

Step 1: A rectangular region B and a mesh size are chosen. A starting point on the boundary of B is chosen.

Step 2: The algorithm advances along the boundary of B, computing L_z at each mesh point of the boundary. The pairs of distinct points are stored along with a direction $\vec{n}$ pointing towards the interior of B. This continues until the algorithm returns back to the starting point.

Step 3: For each triple $(z_1, z_2, \vec{n})$, with (z_1, z_2) being consecutive distinct mesh points on the boundary of B, the algorithm finds another mesh point z_3 inside B, obtained by moving one step from z_2 (on the horizontal sides) or from z_1 (on the vertical sides) in the direction $\vec{n}$, and computes the value L_{z_3}.

Step 4: This triangle has at least one distinct edge (z_1, z_2). If the two other edges are also distinct, a saturated triangle has been found. Otherwise, the algorithm picks up the distinct edge which is not (z_1, z_2) and a new direction $\vec{n}$ as a basis for a new triangle inside B to consider. Thus, the algorithm will proceed along the boundary of two zones associated with two different values, L_z, until either a saturated triangle has been found or a boundary of B is reached again. In the latter case, the next triple $(z_1, z_2, \vec{n})$ on the boundary is picked up and the search continues until all zone boundaries have been traversed.

In the next stage, the algorithm proceeds to a subdivision of saturated triangles by bounding them with rectangles onto which the same algorithm is reapplied. This subdivision is performed several times, until a desired accuracy of approximation is obtained. The centers of saturated triangles then serve as starting points for a refinement via Newton's method.

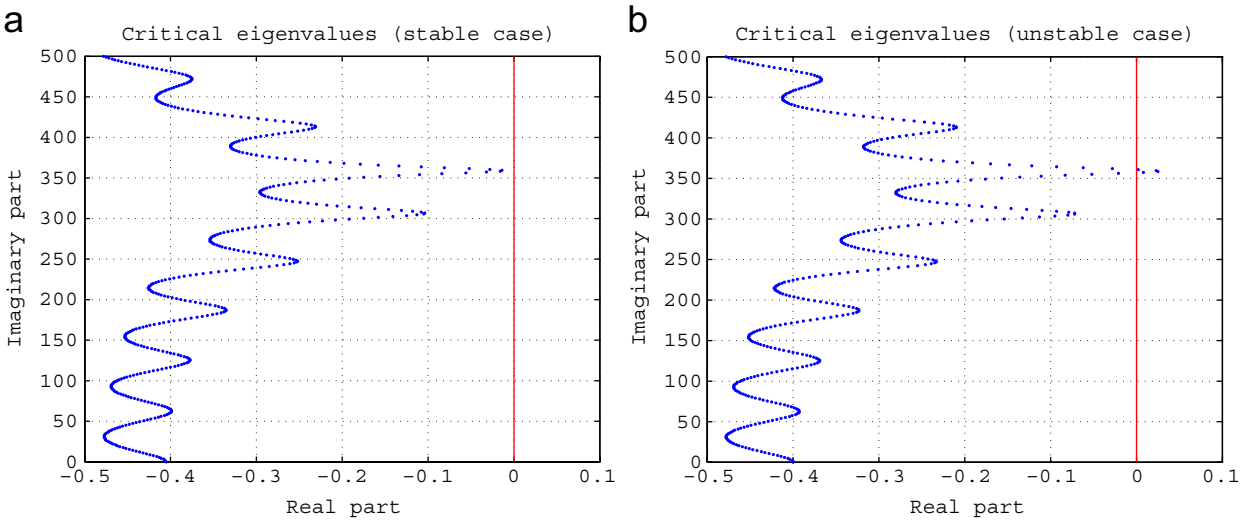

Fig. 4. Location of eigenvalues: (a) stable and (b) unstable cases.

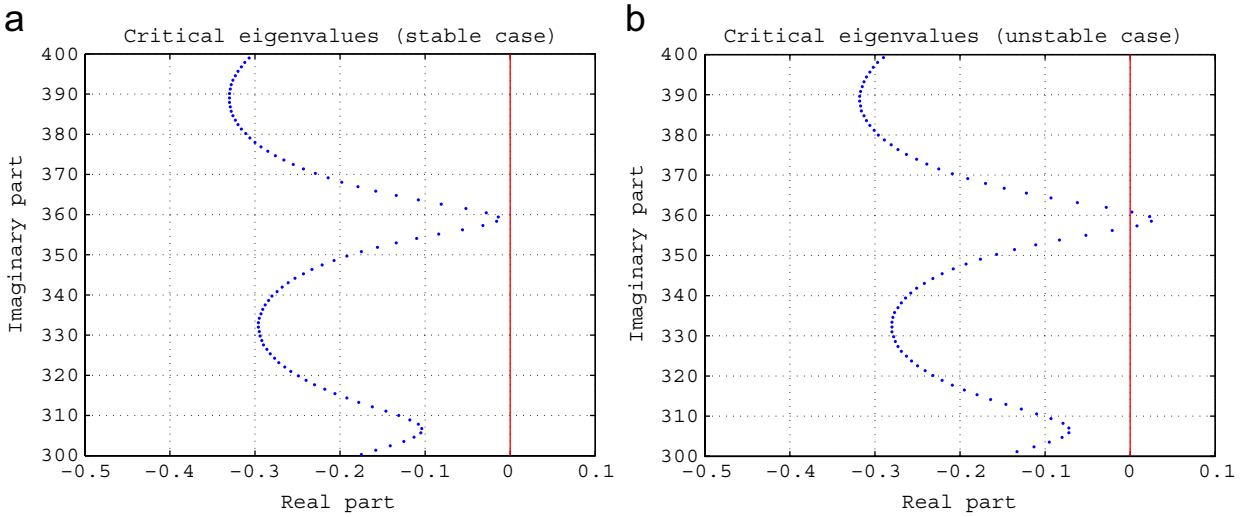

Fig. 5. Critical eigenvalues: (a) stable and (b) unstable cases.

The roots of the function $\Delta(\lambda)$ are plotted in Fig. 4 for the two cases of references described in the last section. The localization of these eigenvalues corroborates the numerical simulations: the stable case (for $\omega_w = 1.1$) corresponds to eigenvalues entirely in the left part of the complex plane. Unstable situations (as for $\omega_w = 1.2$) occur when one or more eigenvalues have crossed the imaginary axis. A close look at the region enclosing the critical eigenvalues for these two cases is presented in Fig. 5. A remark of interest is that this crossing always occurs at or close to a specific value of the imaginary part, corresponding to a sort of critical vibration frequency ($340/6.28 \approx 54$ Hz for the set of physical parameters used in this paper).

In the unstable case (b), there are four eigenvalues on the right part of the complex plane, each of which contributes to the exponential increase of the signal amplitude. The sum of the four real parts ($S = 2.48 \times 10^{-2} + 2.27 \times 10^{-2} + 7.8 \times 10^{-3} + 2.36 \times 10^{-3} = 5.77 \times 10^{-2}$) is close to the value of the Thompson's index a approximated in Section 3.

5. Stability diagrams

During the grinding process, the operator can control the parameters ω_w and ω_g that are associated with the rate of rotation of the workpiece and of the tool as well as the feed velocity v_g and the depth of cut. However, in the present model, the depth of cut is not used in the computation of the system eigenvalues and as a consequence, cannot be used as a control parameter. Therefore, the three parameters $(\omega_w, \omega_g, v_g)$ are the only parameters that can be controlled. Eq. (3) relates the parameters ω_w and v_g to the overlapping coefficient α. This coefficient must satisfy $0 \leqslant \alpha < 1$ as v_g must be greater than 0 (the roll length is much greater than the grinder width), and because all the parts of the roll must be touched by the grinder, v_g cannot be "too large" or ω_w "too small"; they must also obey the constraint $W\omega_w/v_g > 2\pi$.

In this section, we determine the domain of stability of the retarded differential system numerically in the parameter space $(\omega_w, \omega_g, v_g)$. That is done in the following manner: For given values of the three control parameters, let λ_c be the rightmost eigenvalue, and define the real function F by $F(\omega_w, \omega_g, v_g) = \mathrm{Re}(\lambda_c)$ (largest real part of the eigenvalues). The shape of the surface $F = 0$ in the control parameter space will be investigated by drawing sections of this surface in the planes $v_g = C$. Keeping v_g at a fixed value, the parameter, ω_g, successively takes all the values in the range $[30, 90]$ separated by an increment, $\Delta\omega_g = 1$. For each of these values, the equation $F_{v_g,\omega_g}(\omega_w) = 0$ is solved by using the bisection method. In Fig. 6 the stability boundary, $\omega_w = f(\omega_g)$, is plotted for $v_g = 0.01$ m/s, together with the lower limit, $\omega_{w,\min} = 2\pi v_g/W$. For this value of v_g, the operational parameters (ω_w, ω_g) must be kept within the shaded region.

Such sections may be computed for a series of v_g values, and the points $(\omega_w, \omega_g, v_g)$ are then connected to give the spatial curves appearing in Fig. 7. On this figure, the curves represent the upper limit of ω_w for the

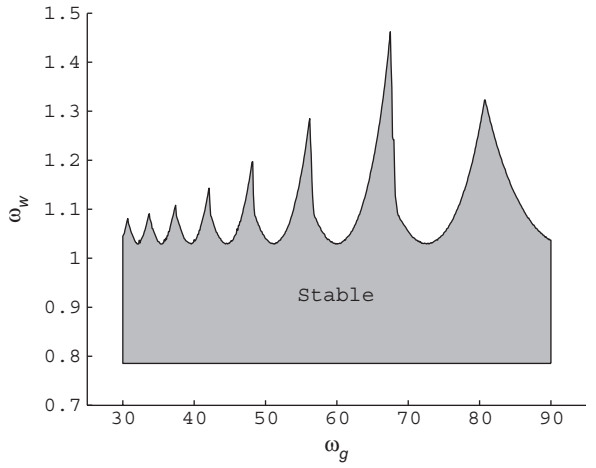

Fig. 6. Smooth grinding region ($v_g = 0.01$ m/s).

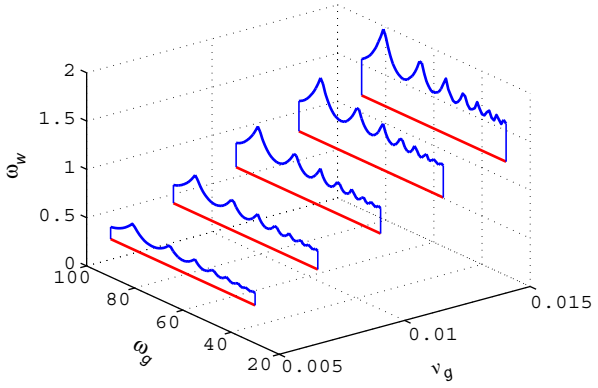

Fig. 7. Sections of the stability boundary surface.

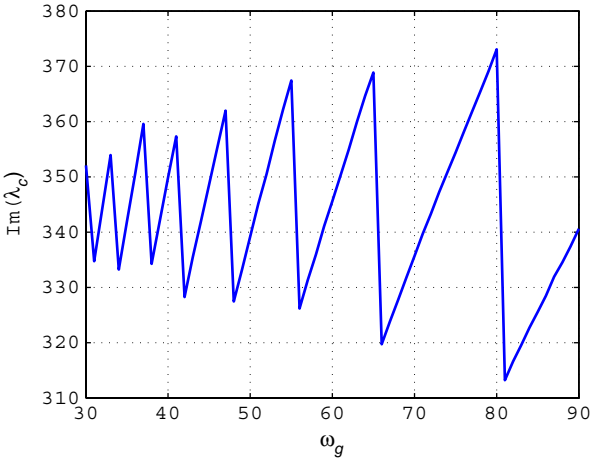

Fig. 8. Imaginary part of the critical eigenvalues.

stability, and the horizontal lines represent the lower admissible value to ensure grinding overlap. In order to grind all parts of the roll without chatter, the system must operate within the region situated above the constraint plane, and below the stability surface.

It can also be seen that the imaginary part of the critical eigenvalues does not depend on the feed velocity v_g. These critical eigenvalues cross the imaginary axis at a height restricted to the range [310, 370] for all the values taken by ω_g (see Fig. 8). This is in accord with previous observations [17] reported in the literature. In Ref. [18], the authors have used this remark to design a chatter monitoring system based on the detection of this critical frequency.

6. Sensitivity analysis on control parameters

In this section, we present an analysis which could enable the setting up of a strategy to prevent the onset of chatter or, in the case where this unstable behavior appears, to bring it to its extinction.

Let us consider a critical situation (stable or unstable) in which the critical eigenvalue λ_c is located close to the imaginary axis. We want to develop a strategy to apply to the control parameters to ensure that this eigenvalue will move towards the left part of the complex plane, which will result in bringing the mechanical system back into a smooth grinding situation. The control parameters $(\omega_w, \omega_g, v_g)$ do not explicitly appear in the coefficients of the system of Eq. (8); however, their expressions may be used directly in Eqs. (11) and (12):

$$\tau_1 = \frac{2\pi}{\omega_g}, \quad \tau_2 = \frac{2\pi}{\omega_w}, \quad \alpha = 1 - \frac{2\pi v_g}{W\omega_w}, \tag{14}$$

which may be re-written as

$$\begin{aligned} \theta_i(\lambda_c) &= T_{i,0} + T_{i,1}\mu_1 + \alpha T_{i,2}\mu_2, \\ \mu_1 &= \exp\left(-\frac{2\pi}{\omega_g}\lambda_c\right), \\ \mu_2 &= \exp\left(-\frac{2\pi}{\omega_w}\lambda_c\right), \end{aligned} \tag{15}$$

where $T_{i,j}$ denote physical values not related to the three control parameters. Let us then evaluate the influence of the parameter ω_w on the critical eigenvalue $\lambda_c(\omega_w)$. Differentiating the identity $\Delta(\lambda_c, \omega_w) = 0$, we obtain

$$\frac{\partial\Delta}{\partial\lambda}\,\mathrm{d}\lambda_c + \frac{\partial\Delta}{\partial\omega_w}\,\mathrm{d}\omega_w = 0 \Rightarrow \frac{\mathrm{d}\lambda_c}{\mathrm{d}\omega_w} = -\frac{\partial\Delta}{\partial\omega_w}\Big/\frac{\partial\Delta}{\partial\lambda}. \tag{16}$$

We then first compute

$$\frac{\partial\Delta}{\partial\lambda} = 4\lambda_c^3 + 3\theta_1\lambda_c^2 + 2\theta_2\lambda_c + \theta_3 - \sum_{i=2}^{4}[\tau_1 T_{i,1}\mu_1 + \alpha\tau_2 T_{i,2}\mu_2]\lambda_c^{4-i} \tag{17}$$

and in a second step

$$\frac{\partial\Delta}{\partial\omega_w} = \sum_{i=2}^{4}\frac{\mathrm{d}\theta_i}{\mathrm{d}\omega_w}\lambda_c^{4-i} = 2\pi\frac{\mu_2}{\omega_w^2}\left[\frac{v_g}{W} + \alpha\lambda_c\right]\sum_{i=2}^{4} T_{i,2}\lambda_c^{4-i}. \tag{18}$$

In a similar manner, we may obtain

$$\begin{aligned} \frac{\mathrm{d}\lambda_c}{\mathrm{d}\omega_g} &= -\frac{\partial\Delta}{\partial\omega_g}\Big/\frac{\partial\Delta}{\partial\lambda}, \\ \frac{\partial\Delta}{\partial\omega_g} &= \sum_{i=2}^{4}\frac{\mathrm{d}\theta_i}{\mathrm{d}\omega_g}\lambda_c^{4-i} = 2\pi\frac{\lambda_c\mu_1}{\omega_g^2}\sum_{i=2}^{4} T_{i,1}\,\lambda_c^{4-i}, \end{aligned} \tag{19}$$

and

$$\frac{\mathrm{d}\lambda_c}{\mathrm{d}v_g} = -\frac{\partial\Delta}{\partial v_g}\Big/\frac{\partial\Delta}{\partial\lambda},$$
$$\frac{\partial\Delta}{\partial v_g} = \sum_{i=2}^{4}\frac{\mathrm{d}\theta_i}{\mathrm{d}v_g}\lambda_c^{4-i} = -2\pi\frac{\mu_2}{W\omega_w}\sum_{i=2}^{4}T_{i,2}\lambda_c^{4-i}. \tag{20}$$

Let us take the reference case previously used as a numerical example: $\omega_w = 1.1, \omega_g = 62.83$ and $v_g = 0.0105$. For these values, the system is close to chatter as the critical eigenvalue $\lambda_c = -0.0142 + \mathrm{i}359.39$. The computation of derivatives results in

$$\frac{\mathrm{d}\lambda_c}{\mathrm{d}\omega_w} = 0.438 - \mathrm{i}8.85,$$
$$\frac{\mathrm{d}\lambda_c}{\mathrm{d}\omega_g} = -0.01275 - \mathrm{i}12.56,$$
$$\frac{\mathrm{d}\lambda_c}{\mathrm{d}v_g} = -51.72 - \mathrm{i}0.174.$$

The signs of these derivatives tell us that for λ_c to move to the left, we must decrease ω_w, or increase ω_g or v_g. Let us modify each of these control parameters independently by a 5% factor. Then, the real part of λ_c will decrease accordingly:

$$\delta\,\mathrm{Re}[\lambda_c(0.95\omega_w)] = -0.024,$$
$$\delta\,\mathrm{Re}[\lambda_c(1.05\omega_g)] = -0.040,$$
$$\delta\,\mathrm{Re}[\lambda_c(1.05v_g)] = -0.027.$$

In this example, the best strategy would be to increase the grinder's rotational velocity, ω_g. The other best control strategies would involve increasing the linear velocity v_g or decreasing the roll rotation ω_w. However, each of these actions would also decrease α: to satisfy the overlapping constraint, the new values v_g^n or ω_w^n must be bound by the inequalities

$$v_g^n \leqslant f v_g \quad \text{or} \quad \omega_w^n \geqslant \frac{1}{f}\omega_w, \tag{21}$$

where

$$f = \frac{W\omega_w}{2\pi v_g}.$$

In practice, this sensitivity analysis could be useful for setting up a method for online chatter monitoring and control.

7. Conclusion

We have presented a systematic approach for the stability analysis of a doubly regenerative cylindrical grinding process. It is known that such a dynamic system with two time delays possesses an infinite number of eigenvalues. We developed an efficient numerical method to locate the rightmost eigenvalue (λ_c) of the system in the complex plane. When λ_c is close to the imaginary axis, its real part indicates the stability state of the system as its imaginary part is related to the chatter frequency. Moreover, the real part of λ_c can be easily related to the chatter growth index introduced by Thompson [3]. Compared to previous research on the kind of system studied here, our approach has the capability of capturing stability characteristics in parameter space directly from the spectrum without using the time-domain response. By using the relationship between the critical eigenvalue and the system parameters, we also conducted a sensitivity analysis in an attempt to find the best control strategy for returning an unstable process to a stable one by varying one of the operational parameters.

Acknowledgments

The authors would like to thank L. Yuan who advised us about some published papers and books on the subject of cylindrical grinding process modeling. The second author of this paper would like also to acknowledge the support provided by the École de Technologie Supérieure.

Appendix

The following nominal values of the physical parameters of the grinding process are used throughout this paper:

$$
\begin{aligned}
&m_1 = 700\ (\mathrm{kg}), \quad m_2 = 400\ (\mathrm{kg}),\\
&c_1 = 6.0 \times 10^4\ (\mathrm{N\,s/m}), \quad c_2 = 3.75 \times 10^4\ (\mathrm{N\,s/m}),\\
&k_1 = 4.0 \times 10^7\ (\mathrm{N/m}), \quad k_2 = 2.5 \times 10^7\ (\mathrm{N/m}),\\
&k_N = 1.6 \times 10^7\ (\mathrm{N/m}), \quad W = 0.08\ (\mathrm{m}),\\
&\Delta_R = 2.0 \times 10^{-4}\ (\mathrm{m}), \quad \Delta_r = 1.0 \times 10^{-4}\ (\mathrm{m}),\\
&n_w = 10, \quad n_g = 10,\\
&x_{f_w} = 1.0 \times 10^{-6}\ (\mathrm{m}).
\end{aligned}
$$

The rotational and axial velocities of the reference case correspond to

$$v_g = 0.0105\ (\mathrm{m/s}), \quad \omega_g = 62.83\ (\mathrm{rad/s}), \quad \omega_w = 1.1\,(\mathrm{rad/s}).$$

References

[1] M.A. Davies, Dynamic problems in hard-turning, milling, and grinding, in: C.M. Francis (Ed.), *Dynamics and Chaos in Manufacturing Processes*, Wiley, New york, 1998, pp. 57–91.
[2] R.A. Thompson, On the double regenerative stability of a grinder, *ASME Journal of Engineering for Industry Serie B* 96 (1) (1974) 275–280.
[3] R.A. Thompson, On the double regenerative stability of a grinder: the theory of chatter growth, *ASME Journal of Engineering for Industry Serie B* 108 (2) (1986) 75–82.
[4] R.A. Thompson, On the double regenerative stability of a grinder: the mathematical analysis of chatter growth, *ASME Journal of Engineering for Industry Serie B* 108 (2) (1986) 83–92.
[5] R.A. Thompson, On the double regenerative stability of a grinder: the effect of contact stifness and wave filtering, *ASME Journal of Engineering for Industry Serie B* 114 (1) (1992) 53–60.
[6] L. Yuan, V.-M. Järvenpää, E. Keskinen, M. Cotsaftis, Simulation of roll grinding system dynamics with rotor and speed control, *Communications in Nonlinear Science and Numerical Simulation* 7 (2002) 95–106.
[7] L. Yuan, V.-M. Järvenpää, E. Keskinen, Analysis and simulation of roll grinding system with double time delay effect, *Proceedings of Surveillance*, vol. 5, CETIM, Senlis, France, October 11–13, 2004, pp. 1–11.
[8] L. Yuan, V.-M. Järvenpää, E. Keskinen, M. Cotsaftis, Evaluation of analysis methods for delay differential equations in case study of roll grinding dynamics, *Proceedings of Fifth ASME Biennial Conference on Engineering Systems Design and Analysis*, Montreaux, Switzerland, July 10–13, 2000, pp. 307–312.
[9] L. Yuan, V.-M. Järvenpää, E. Keskinen, M. Cotsaftis, Response and analysis of multi-degree-of-freedom cylindrical roll crinding system, *Proceedings of the Institution of Mechanical Engineers Part K: Journal of Multi-body Dynamics* 216 (4) (2002) 315–325 (ISSN 1464-4193).
[10] M.S. Fofana, Effect of regenerative process on the sample stability of a multiple delay differential equation, *Chaos, Solitons and Fractals* 14 (2002) 301–309.
[11] F. Orynski, W. Pawlowski, Simulation and experimental research of the Grinder's Wheelhead dynamics, *Journal of Vibration and Control* 10 (2004) 915–930.
[12] J. Bélaire, S.A. Campbell, Stability and bifurcations of equilibria in a multiple-delayed differential equation, *SIAM Journal on Applied Mathematics* 54 (5) (1994) 1402–1424.
[13] H.Y. Hu, Z.H. Wang, Stability analysis of damped SDOF systems with two time delays in state feedback, *Journal of Sound and Vibration* 214 (2) (1998) 213–225.
[14] K. Engelborghs, T. Luzyanina, D. Roose, Numerical bifurcation analysis of delay differential equations using DDE-BIFTOOL, *ACM Transactions on Mathematical Software* 28 (1) (2002) 1–21.

[15] A. Manitius, H. Tran, G. Payre, R. Roy, Computation of eigenvalues associated with functional differential equations, *SIAM Journal on Statistical Computation* 8 (3) (1987) 222–246.
[16] Z. Liu, G. Payre, P. Bourassa, Stability and oscillations in a time-delayed vehicle system with driver control, *Nonlinear Dynamics* 35 (2) (2004) 159–173.
[17] B.R. Hardwick, Identification and solution of chatter vibration on roll grinding machines, *Iron and Steel Engineer* (July) (1994) 41–46.
[18] E. Govekar, A. Baus, J. Gradisek, F. Klocke, I. Grabec, A new method for chatter detection in grinding, *CIRP Annals* STC G, 51/1/2002 (2002) 267–270.